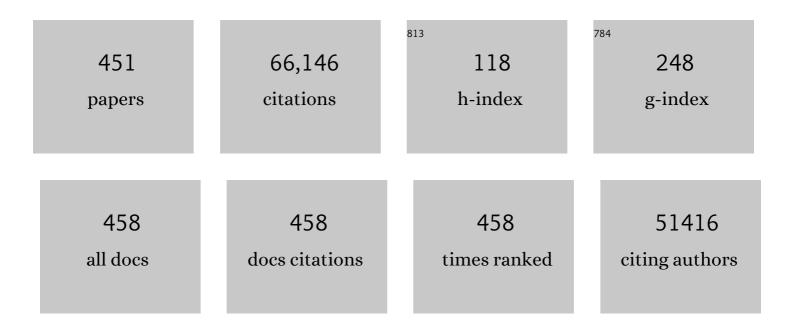
List of Publications by Year in descending order

Source: https://exaly.com/author-pdf/4339592/publications.pdf Version: 2024-02-01



#	Article	IF	CITATIONS
1	The chemistry of two-dimensional layered transition metal dichalcogenide nanosheets. Nature Chemistry, 2013, 5, 263-275.	13.6	8,051
2	Synthesis of Largeâ€Area MoS ₂ Atomic Layers with Chemical Vapor Deposition. Advanced Materials, 2012, 24, 2320-2325.	21.0	2,956
3	Growth of Large-Area and Highly Crystalline MoS ₂ Thin Layers on Insulating Substrates. Nano Letters, 2012, 12, 1538-1544.	9.1	1,749
4	Integrated Circuits Based on Bilayer MoS ₂ Transistors. Nano Letters, 2012, 12, 4674-4680.	9.1	1,526
5	Janus monolayers of transition metal dichalcogenides. Nature Nanotechnology, 2017, 12, 744-749.	31.5	1,459
6	Monolayer MoS ₂ Heterojunction Solar Cells. ACS Nano, 2014, 8, 8317-8322.	14.6	1,081
7	Synthesis of Few-Layer Hexagonal Boron Nitride Thin Film by Chemical Vapor Deposition. Nano Letters, 2010, 10, 4134-4139.	9.1	1,058
8	Epitaxial growth of a monolayer WSe ₂ -MoS ₂ lateral p-n junction with an atomically sharp interface. Science, 2015, 349, 524-528.	12.6	1,009
9	Graphene and two-dimensional materials for silicon technology. Nature, 2019, 573, 507-518.	27.8	936
10	High-Quality Thin Graphene Films from Fast Electrochemical Exfoliation. ACS Nano, 2011, 5, 2332-2339.	14.6	896
11	Highâ€Gain Phototransistors Based on a CVD MoS ₂ Monolayer. Advanced Materials, 2013, 25, 3456-3461.	21.0	891
12	van der Waals Epitaxy of MoS ₂ Layers Using Graphene As Growth Templates. Nano Letters, 2012, 12, 2784-2791.	9.1	888
13	Large-Area Synthesis of Highly Crystalline WSe ₂ Monolayers and Device Applications. ACS Nano, 2014, 8, 923-930.	14.6	885
14	Ultrahigh-Gain Photodetectors Based on Atomically Thin Graphene-MoS2 Heterostructures. Scientific Reports, 2014, 4, 3826.	3.3	771
15	Highly Flexible MoS ₂ Thin-Film Transistors with Ion Gel Dielectrics. Nano Letters, 2012, 12, 4013-4017.	9.1	746
16	Recent advances in controlled synthesis of two-dimensional transition metal dichalcogenides via vapour deposition techniques. Chemical Society Reviews, 2015, 44, 2744-2756.	38.1	709
17	Highly Efficient Electrocatalytic Hydrogen Production by MoS <i>_x</i> Grown on Grapheneâ€Protected 3D Ni Foams. Advanced Materials, 2013, 25, 756-760.	21.0	693
18	Wafer-scale MoS2 thin layers prepared by MoO3 sulfurization. Nanoscale, 2012, 4, 6637.	5.6	621

#	Article	IF	CITATIONS
19	Synthesis and Transfer of Single-Layer Transition Metal Disulfides on Diverse Surfaces. Nano Letters, 2013, 13, 1852-1857.	9.1	612
20	Few-Layer MoS ₂ with High Broadband Photogain and Fast Optical Switching for Use in Harsh Environments. ACS Nano, 2013, 7, 3905-3911.	14.6	584
21	Ultralow contact resistance between semimetal and monolayer semiconductors. Nature, 2021, 593, 211-217.	27.8	579
22	Exceptional Tunability of Band Energy in a Compressively Strained Trilayer MoS ₂ Sheet. ACS Nano, 2013, 7, 7126-7131.	14.6	550
23	Doping Single‣ayer Graphene with Aromatic Molecules. Small, 2009, 5, 1422-1426.	10.0	537
24	Determination of band alignment in the single-layer MoS2/WSe2 heterojunction. Nature Communications, 2015, 6, 7666.	12.8	524
25	Electrical Detection of DNA Hybridization with Singleâ€Base Specificity Using Transistors Based on CVDâ€Grown Graphene Sheets. Advanced Materials, 2010, 22, 1649-1653.	21.0	516
26	Monolayer MoSe ₂ Grown by Chemical Vapor Deposition for Fast Photodetection. ACS Nano, 2014, 8, 8582-8590.	14.6	515
27	Intercorrelated In-Plane and Out-of-Plane Ferroelectricity in Ultrathin Two-Dimensional Layered Semiconductor In ₂ Se ₃ . Nano Letters, 2018, 18, 1253-1258.	9.1	509
28	Work Function Engineering of Graphene Electrode <i>via</i> Chemical Doping. ACS Nano, 2010, 4, 2689-2694.	14.6	501
29	Graphene-modified LiFePO4 cathode for lithium ion battery beyond theoretical capacity. Nature Communications, 2013, 4, 1687.	12.8	481
30	Electrical and Spectroscopic Characterizations of Ultra-Large Reduced Graphene Oxide Monolayers. Chemistry of Materials, 2009, 21, 5674-5680.	6.7	476
31	Heterostructures based on two-dimensional layered materials and their potential applications. Materials Today, 2016, 19, 322-335.	14.2	469
32	Strain engineering and epitaxial stabilization of halide perovskites. Nature, 2020, 577, 209-215.	27.8	417
33	Interlayer couplings, Moiré patterns, and 2D electronic superlattices in MoS ₂ /WSe ₂ hetero-bilayers. Science Advances, 2017, 3, e1601459.	10.3	414
34	Wafer-scale single-crystal hexagonal boron nitride monolayers on CuÂ(111). Nature, 2020, 579, 219-223.	27.8	409
35	Nanoelectronic biosensors based on CVD grown graphene. Nanoscale, 2010, 2, 1485.	5.6	408
36	Intrinsic homogeneous linewidth and broadening mechanisms of excitons in monolayer transition metal dichalcogenides. Nature Communications, 2015, 6, 8315.	12.8	408

#	Article	IF	CITATIONS
37	Direct Imaging of Band Profile in Single Layer MoS ₂ on Graphite: Quasiparticle Energy Gap, Metallic Edge States, and Edge Band Bending. Nano Letters, 2014, 14, 2443-2447.	9.1	402
38	Heterostructured WS ₂ /CH ₃ NH ₃ PbI ₃ Photoconductors with Suppressed Dark Current and Enhanced Photodetectivity. Advanced Materials, 2016, 28, 3683-3689.	21.0	396
39	Second Harmonic Generation from Artificially Stacked Transition Metal Dichalcogenide Twisted Bilayers. ACS Nano, 2014, 8, 2951-2958.	14.6	388
40	Atomically thin resonant tunnel diodes built from synthetic van der Waals heterostructures. Nature Communications, 2015, 6, 7311.	12.8	382
41	Selective Decoration of Au Nanoparticles on Monolayer MoS2 Single Crystals. Scientific Reports, 2013, 3, 1839.	3.3	380
42	Role of Metal Contacts in High-Performance Phototransistors Based on WSe ₂ Monolayers. ACS Nano, 2014, 8, 8653-8661.	14.6	380
43	Bandgap tunability at single-layer molybdenum disulphide grain boundaries. Nature Communications, 2015, 6, 6298.	12.8	358
44	CoP nanosheet assembly grown on carbon cloth: A highly efficient electrocatalyst for hydrogen generation. Nano Energy, 2015, 15, 634-641.	16.0	357
45	Graphene-based biosensors for detection of bacteria and their metabolic activities. Journal of Materials Chemistry, 2011, 21, 12358.	6.7	343
46	Transistors based on two-dimensional materials for future integrated circuits. Nature Electronics, 2021, 4, 786-799.	26.0	335
47	Enhancing the conductivity of transparent graphene films via doping. Nanotechnology, 2010, 21, 285205.	2.6	321
48	Optical properties of monolayer transition metal dichalcogenides probed by spectroscopic ellipsometry. Applied Physics Letters, 2014, 105, .	3.3	317
49	Toward the Extraction of Single Species of Single-Walled Carbon Nanotubes Using Fluorene-Based Polymers. Nano Letters, 2007, 7, 3013-3017.	9.1	314
50	Direct Formation of Wafer Scale Graphene Thin Layers on Insulating Substrates by Chemical Vapor Deposition. Nano Letters, 2011, 11, 3612-3616.	9.1	302
51	Self-assembly of hierarchical MoSx/CNT nanocomposites (2 <x<3): 2013,="" 2169.<="" 3,="" anode="" batteries.="" for="" high="" ion="" lithium="" materials="" performance="" reports,="" scientific="" td="" towards=""><td>3.3</td><td>290</td></x<3):>	3.3	290
52	Graphene/MoS ₂ Heterostructures for Ultrasensitive Detection of DNA Hybridisation. Advanced Materials, 2014, 26, 4838-4844.	21.0	290
53	Spectroscopic Signatures for Interlayer Coupling in MoS ₂ –WSe ₂ van der Waals Stacking. ACS Nano, 2014, 8, 9649-9656.	14.6	288
54	Epitaxial Growth of Two-Dimensional Layered Transition-Metal Dichalcogenides: Growth Mechanism, Controllability, and Scalability. Chemical Reviews, 2018, 118, 6134-6150.	47.7	285

#	Article	IF	CITATIONS
55	Pressure-Dependent Optical and Vibrational Properties of Monolayer Molybdenum Disulfide. Nano Letters, 2015, 15, 346-353.	9.1	284
56	Recent Progress on Two-Dimensional Materials. Wuli Huaxue Xuebao/ Acta Physico - Chimica Sinica, 2021, .	4.9	269
57	Nitrogen-Doped Graphene Sheets Grown by Chemical Vapor Deposition: Synthesis and Influence of Nitrogen Impurities on Carrier Transport. ACS Nano, 2013, 7, 6522-6532.	14.6	264
58	Ultrafast generation of pseudo-magnetic field for valley excitons in WSe ₂ monolayers. Science, 2014, 346, 1205-1208.	12.6	261
59	Two-dimensional materials with piezoelectric and ferroelectric functionalities. Npj 2D Materials and Applications, 2018, 2, .	7.9	258
60	Strong Rashba-Edelstein Effect-Induced Spin–Orbit Torques in Monolayer Transition Metal Dichalcogenide/Ferromagnet Bilayers. Nano Letters, 2016, 16, 7514-7520.	9.1	247
61	Diameter-selective encapsulation of metallocenes in single-walled carbon nanotubes. Nature Materials, 2005, 4, 481-485.	27.5	245
62	Giant photoluminescence enhancement in tungsten-diselenide–gold plasmonic hybrid structures. Nature Communications, 2016, 7, 11283.	12.8	244
63	Highly Efficient Restoration of Graphitic Structure in Graphene Oxide Using Alcohol Vapors. ACS Nano, 2010, 4, 5285-5292.	14.6	242
64	Roomâ€Temperature Ferroelectricity in Hexagonally Layered αâ€In ₂ Se ₃ Nanoflakes down to the Monolayer Limit. Advanced Functional Materials, 2018, 28, 1803738.	14.9	241
65	Emerging energy applications of two-dimensionalÂlayered transition metal dichalcogenides. Nano Energy, 2015, 18, 293-305.	16.0	236
66	Mode locking of ceramic Nd:yttrium aluminum garnet with graphene as a saturable absorber. Applied Physics Letters, 2010, 96, .	3.3	234
67	Piezoelectric effect in chemical vapour deposition-grown atomic-monolayer triangular molybdenum disulfide piezotronics. Nature Communications, 2015, 6, 7430.	12.8	233
68	Metal–Organic Framework-Based Separators for Enhancing Li–S Battery Stability: Mechanism of Mitigating Polysulfide Diffusion. ACS Energy Letters, 2017, 2, 2362-2367.	17.4	229
69	Symmetry Breaking of Graphene Monolayers by Molecular Decoration. Physical Review Letters, 2009, 102, 135501.	7.8	224
70	Recognizing the Mechanism of Sulfurized Polyacrylonitrile Cathode Materials for Li–S Batteries and beyond in Al–S Batteries. ACS Energy Letters, 2018, 3, 2899-2907.	17.4	224
71	Direct measurement of exciton valley coherence in monolayer WSe2. Nature Physics, 2016, 12, 677-682.	16.7	223
72	Opening an Electrical Band Gap of Bilayer Graphene with Molecular Doping. ACS Nano, 2011, 5, 7517-7524.	14.6	222

#	Article	IF	CITATIONS
73	How 2D semiconductors could extend Moore's law. Nature, 2019, 567, 169-170.	27.8	222
74	Observation of chiral phonons. Science, 2018, 359, 579-582.	12.6	217
75	New Insights on Graphite Anode Stability in Rechargeable Batteries: Li Ion Coordination Structures Prevail over Solid Electrolyte Interphases. ACS Energy Letters, 2018, 3, 335-340.	17.4	217
76	Multidirection Piezoelectricity in Mono- and Multilayered Hexagonal α-In ₂ Se ₃ . ACS Nano, 2018, 12, 4976-4983.	14.6	215
77	Strain distributions and their influence on electronic structures of WSe2–MoS2 laterally strained heterojunctions. Nature Nanotechnology, 2018, 13, 152-158.	31.5	206
78	Layer-by-Layer Graphene/TCNQ Stacked Films as Conducting Anodes for Organic Solar Cells. ACS Nano, 2012, 6, 5031-5039.	14.6	199
79	Nitrogen-Doped Nanoporous Carbon Membranes with Co/CoP Janus-Type Nanocrystals as Hydrogen Evolution Electrode in Both Acidic and Alkaline Environments. ACS Nano, 2017, 11, 4358-4364.	14.6	199
80	Enhanced Thermoelectric Performance of PEDOT:PSS Flexible Bulky Papers by Treatment with Secondary Dopants. ACS Applied Materials & Interfaces, 2015, 7, 94-100.	8.0	194
81	Extraordinarily Stretchable Allâ€Carbon Collaborative Nanoarchitectures for Epidermal Sensors. Advanced Materials, 2017, 29, 1606411.	21.0	194
82	Comparative study on MoS2 and WS2 for electrocatalytic water splitting. International Journal of Hydrogen Energy, 2013, 38, 12302-12309.	7.1	193
83	Ultrafast Transient Terahertz Conductivity of Monolayer MoS ₂ and WSe ₂ Grown by Chemical Vapor Deposition. ACS Nano, 2014, 8, 11147-11153.	14.6	191
84	Highly acid-durable carbon coated Co3O4 nanoarrays as efficient oxygen evolution electrocatalysts. Nano Energy, 2016, 25, 42-50.	16.0	187
85	Label-free detection of DNA hybridization using transistors based on CVD grown graphene. Biosensors and Bioelectronics, 2013, 41, 103-109.	10.1	185
86	(n,m) Selectivity of Single-Walled Carbon Nanotubes by Different Carbon Precursors on Coâ^'Mo Catalysts. Journal of the American Chemical Society, 2007, 129, 9014-9019.	13.7	184
87	One-step growth of graphene–carbon nanotube hybrid materials by chemical vapor deposition. Carbon, 2011, 49, 2944-2949.	10.3	182
88	Enhanced Thermopower of Graphene Films with Oxygen Plasma Treatment. ACS Nano, 2011, 5, 2749-2755.	14.6	181
89	Graphene-Based High-Efficiency Surface-Enhanced Raman Scattering-Active Platform for Sensitive and Multiplex DNA Detection. Analytical Chemistry, 2012, 84, 4622-4627.	6.5	180
90	Photoluminescence Enhancement and Structure Repairing of Monolayer MoSe ₂ by Hydrohalic Acid Treatment. ACS Nano, 2016, 10, 1454-1461.	14.6	179

#	Article	IF	CITATIONS
91	Highâ€Sulfurâ€Vacancy Amorphous Molybdenum Sulfide as a High Current Electrocatalyst in Hydrogen Evolution. Small, 2016, 12, 5530-5537.	10.0	177
92	Ultra-large single-layer graphene obtained from solution chemical reduction and its electrical properties. Physical Chemistry Chemical Physics, 2010, 12, 2164.	2.8	176
93	Probing Critical Point Energies of Transition Metal Dichalcogenides: Surprising Indirect Gap of Single Layer WSe ₂ . Nano Letters, 2015, 15, 6494-6500.	9.1	175
94	Stable mode-locked fiber laser based on CVD fabricated graphene saturable absorber. Optics Express, 2012, 20, 2460.	3.4	174
95	Effective doping of single-layer graphene from underlying < mml:math xmlns:mml="http://www.w3.org/1998/Math/MathML" display="inline" > < mml:mrow > < mml:mrow > < mml:mtext > SiO < / mml:mtext > < / mml:mrow > < mml:mn > 2 Physical Review B, 2009, 79	2< <mark>3¦2</mark> mml:m	173 in>
96	Defect Structure of Localized Excitons in a <mml:math xmlns:mml="http://www.w3.org/1998/Math/MathML" display="inline"><mml:mrow><mml:msub><mml:mrow><mml:mi>WSe</mml:mi></mml:mrow><mml:mn>2Monolayer. Physical Review Letters, 2017, 119, 046101.</mml:mn></mml:msub></mml:mrow></mml:math 	ml ?n8 n> <td>nml:msub><!--</td--></td>	nml:msub> </td
97	New Insight on the Role of Electrolyte Additives in Rechargeable Lithium Ion Batteries. ACS Energy Letters, 2019, 4, 2613-2622.	17.4	160
98	Growth of large-sized graphene thin-films by liquid precursor-based chemical vapor deposition under atmospheric pressure. Carbon, 2011, 49, 3672-3678.	10.3	158
99	Using oxidation to increase the electrical conductivity of carbon nanotube electrodes. Carbon, 2009, 47, 1867-1870.	10.3	152
100	Optically initialized robust valley-polarized holes in monolayer WSe2. Nature Communications, 2015, 6, 8963.	12.8	151
101	Three-Dimensional Heterostructures of MoS ₂ Nanosheets on Conducting MoO ₂ as an Efficient Electrocatalyst To Enhance Hydrogen Evolution Reaction. ACS Applied Materials & Interfaces, 2015, 7, 23328-23335.	8.0	150
102	Interfacing Glycosylated Carbonâ€Nanotubeâ€Network Devices with Living Cells to Detect Dynamic Secretion of Biomolecules. Angewandte Chemie - International Edition, 2009, 48, 2723-2726.	13.8	148
103	Fluorinated Graphene as High Performance Dielectric Materials and the Applications for Graphene Nanoelectronics. Scientific Reports, 2014, 4, 5893.	3.3	147
104	DNA Sensing by Field-Effect Transistors Based on Networks of Carbon Nanotubes. Journal of the American Chemical Society, 2007, 129, 14427-14432.	13.7	144
105	Synthesis of single-crystal-like nanoporous carbon membranes and their application in overall water splitting. Nature Communications, 2017, 8, 13592.	12.8	142
106	Direct determination of monolayer MoS ₂ and WSe ₂ exciton binding energies on insulating and metallic substrates. 2D Materials, 2018, 5, 025003.	4.4	142
107	Photoelectrical Response in Singleâ€Layer Graphene Transistors. Small, 2009, 5, 2005-2011.	10.0	141
108	One-step synthesis of single-site vanadium substitution in 1T-WS2 monolayers for enhanced hydrogen evolution catalysis. Nature Communications, 2021, 12, 709.	12.8	137

#	Article	IF	CITATIONS
109	Activating basal-plane catalytic activity of two-dimensional MoS2 monolayer with remote hydrogen plasma. Nano Energy, 2016, 30, 846-852.	16.0	136
110	Hole mobility enhancement and <i>p</i> -doping in monolayer WSe ₂ by gold decoration. 2D Materials, 2014, 1, 034001.	4.4	134
111	Novel Field-Effect Schottky Barrier Transistors Based on Graphene-MoS2 Heterojunctions. Scientific Reports, 2014, 4, 5951.	3.3	134
112	Rugae-like FeP nanocrystal assembly on a carbon cloth: an exceptionally efficient and stable cathode for hydrogen evolution. Nanoscale, 2015, 7, 10974-10981.	5.6	133
113	Atomically Thin Heterostructures Based on Single-Layer Tungsten Diselenide and Graphene. Nano Letters, 2014, 14, 6936-6941.	9.1	132
114	MXene based self-assembled cathode and antifouling separator for high-rate and dendrite-inhibited Li–S battery. Nano Energy, 2019, 61, 478-485.	16.0	131
115	Point Defects and Localized Excitons in 2D WSe ₂ . ACS Nano, 2019, 13, 6050-6059.	14.6	127
116	Formation of Segregation Morphology in Crystalline/Amorphous Polymer Blends:Â Molecular Weight Effect. Macromolecules, 1998, 31, 2255-2264.	4.8	123
117	Bidirectional Allâ€Optical Synapses Based on a 2D Bi ₂ O ₂ Se/Graphene Hybrid Structure for Multifunctional Optoelectronics. Advanced Functional Materials, 2020, 30, 2001598.	14.9	123
118	Gateâ€Tunable and Multidirectionâ€Switchable Memristive Phenomena in a Van Der Waals Ferroelectric. Advanced Materials, 2019, 31, e1901300.	21.0	121
119	Extreme sensitivity of graphene photoconductivity to environmental gases. Nature Communications, 2012, 3, 1228.	12.8	120
120	Visualizing band offsets and edge states in bilayer–monolayer transition metal dichalcogenides lateral heterojunction. Nature Communications, 2016, 7, 10349.	12.8	120
121	Selective Synthesis of (9,8) Single Walled Carbon Nanotubes on Cobalt Incorporated TUD-1 Catalysts. Journal of the American Chemical Society, 2010, 132, 16747-16749.	13.7	119
122	<mml:math <br="" xmlns:mml="http://www.w3.org/1998/Math/MathML">display="inline"><mml:mi>G</mml:mi></mml:math> -band Raman double resonance in twisted bilayer graphene: Evidence of band splitting and folding. Physical Review B, 2009, 80, .	3.2	116
123	Symmetrical synergy of hybrid Co9S8-MoSx electrocatalysts for hydrogen evolution reaction. Nano Energy, 2017, 32, 470-478.	16.0	116
124	Labelâ€Free Electrical Detection of DNA Hybridization on Graphene using Hall Effect Measurements: Revisiting the Sensing Mechanism. Advanced Functional Materials, 2013, 23, 2301-2307.	14.9	114
125	Synthesis and Characterization of New Soluble Polyimides from 3,3â€~,4,4â€~-Benzhydrol Tetracarboxylic Dianhydride and Various Diamines. Chemistry of Materials, 1998, 10, 734-739.	6.7	113
126	Observing Grain Boundaries in CVD-Grown Monolayer Transition Metal Dichalcogenides. ACS Nano, 2014, 8, 11401-11408.	14.6	113

#	Article	IF	CITATIONS
127	Highly Flexible and Highâ€Performance Complementary Inverters of Largeâ€Area Transition Metal Dichalcogenide Monolayers. Advanced Materials, 2016, 28, 4111-4119.	21.0	112
128	Single Atomically Sharp Lateral Monolayer pâ€n Heterojunction Solar Cells with Extraordinarily High Power Conversion Efficiency. Advanced Materials, 2017, 29, 1701168.	21.0	111
129	Band Gapâ€Tunable Molybdenum Sulfide Selenide Monolayer Alloy. Small, 2014, 10, 2589-2594.	10.0	109
130	Colorless-to-colorful switching electrochromic polyimides with very high contrast ratio. Nature Communications, 2019, 10, 1239.	12.8	109
131	High-κ perovskite membranes as insulators for two-dimensional transistors. Nature, 2022, 605, 262-267.	27.8	109
132	Synergistic additive-mediated CVD growth and chemical modification of 2D materials. Chemical Society Reviews, 2019, 48, 4639-4654.	38.1	108
133	Structurally Deformed MoS ₂ for Electrochemically Stable, Thermally Resistant, and Highly Efficient Hydrogen Evolution Reaction. Advanced Materials, 2017, 29, 1703863.	21.0	107
134	Two-dimensional materials for electronic applications. MRS Bulletin, 2014, 39, 711-718.	3.5	104
135	Ledge-directed epitaxy of continuously self-aligned single-crystalline nanoribbons of transition metal dichalcogenides. Nature Materials, 2020, 19, 1300-1306.	27.5	104
136	Spherulitic Crystallization Behavior of Poly(ε-caprolactone) with a Wide Range of Molecular Weight. Macromolecules, 1997, 30, 1718-1722.	4.8	102
137	Plasmonic Gold Nanorods Coverage Influence on Enhancement of the Photoluminescence of Two-Dimensional MoS2 Monolayer. Scientific Reports, 2015, 5, 16374.	3.3	102
138	Substrate Lattice-Guided Seed Formation Controls the Orientation of 2D Transition-Metal Dichalcogenides. ACS Nano, 2017, 11, 9215-9222.	14.6	102
139	Converting Graphene Oxide Monolayers into Boron Carbonitride Nanosheets by Substitutional Doping. Small, 2012, 8, 1384-1391.	10.0	101
140	Molybdenum Sulfide Supported on Crumpled Graphene Balls for Electrocatalytic Hydrogen Production. Advanced Energy Materials, 2014, 4, 1400398.	19.5	101
141	Low overpotential and high current CO2 reduction with surface reconstructed Cu foam electrodes. Nano Energy, 2016, 27, 121-129.	16.0	100
142	Lithiumâ€lon Desolvation Induced by Nitrate Additives Reveals New Insights into High Performance Lithium Batteries. Advanced Functional Materials, 2021, 31, 2101593.	14.9	100
143	Evidence of indirect gap in monolayer WSe2. Nature Communications, 2017, 8, 929.	12.8	98
144	Selectively Plasmon-Enhanced Second-Harmonic Generation from Monolayer Tungsten Diselenide on Flexible Substrates. ACS Nano, 2018, 12, 1859-1867.	14.6	97

#	Article	IF	CITATIONS
145	Sub-nanometre channels embedded in two-dimensional materials. Nature Materials, 2018, 17, 129-133.	27.5	97
146	Electrical Detection of Femtomolar DNA via Goldâ€Nanoparticle Enhancement in Carbonâ€Nanotubeâ€Network Fieldâ€Effect Transistors. Advanced Materials, 2008, 20, 2389-2393.	21.0	96
147	Fabrication of stretchable MoS2 thin-film transistors using elastic ion-gel gate dielectrics. Applied Physics Letters, 2013, 103, .	3.3	96
148	Comparative studies on acid and thermal based selective purification of HiPCO produced single-walled carbon nanotubes. Chemical Physics Letters, 2004, 386, 239-243.	2.6	95
149	Multilayer Graphene–WSe ₂ Heterostructures for WSe ₂ Transistors. ACS Nano, 2017, 11, 12817-12823.	14.6	95
150	Cellular behavior of human mesenchymal stem cells cultured on single-walled carbon nanotube film. Carbon, 2010, 48, 1095-1104.	10.3	94
151	Direct electrochemistry-based hydrogen peroxide biosensor formed from single-layer graphene nanoplatelet–enzyme composite film. Talanta, 2010, 82, 1344-1348.	5.5	90
152	Negative circular polarization emissions from WSe2/MoSe2 commensurate heterobilayers. Nature Communications, 2018, 9, 1356.	12.8	88
153	Heterointerface Screening Effects between Organic Monolayers and Monolayer Transition Metal Dichalcogenides. ACS Nano, 2016, 10, 2476-2484.	14.6	87
154	A flexible hydrophilic-modified graphene microprobe for neural and cardiac recording. Nanomedicine: Nanotechnology, Biology, and Medicine, 2013, 9, 600-604.	3.3	86
155	Bifunctional separator as a polysulfide mediator for highly stable Li–S batteries. Journal of Materials Chemistry A, 2016, 4, 9661-9669.	10.3	86
156	Observation of Switchable Photoresponse of a Monolayer WSe ₂ –MoS ₂ Lateral Heterostructure via Photocurrent Spectral Atomic Force Microscopic Imaging. Nano Letters, 2016, 16, 3571-3577.	9.1	86
157	Differentiation of Gas Molecules Using Flexible and All-Carbon Nanotube Devices. Journal of Physical Chemistry C, 2008, 112, 650-653.	3.1	85
158	Band Gap Tuning of Graphene by Adsorption of Aromatic Molecules. Journal of Physical Chemistry C, 2012, 116, 13788-13794.	3.1	85
159	Layered Semiconducting 2D Materials for Future Transistor Applications. Small Structures, 2021, 2, 2000103.	12.0	85
160	Controllable Synthesis of Band-Gap-Tunable and Monolayer Transition-Metal Dichalcogenide Alloys. Frontiers in Energy Research, 2014, 2, .	2.3	84
161	Multilayer Approach for Advanced Hybrid Lithium Battery. ACS Nano, 2016, 10, 6037-6044.	14.6	83
162	Decoupling of CVD graphene by controlled oxidation of recrystallized Cu. RSC Advances, 2012, 2, 3008.	3.6	82

#	Article	IF	CITATIONS
163	Threeâ€Dimensional Molybdenum Sulfide Sponges for Electrocatalytic Water Splitting. Small, 2014, 10, 895-900.	10.0	82
164	Symmetric synergy of hybrid CoS ₂ –WS ₂ electrocatalysts for the hydrogen evolution reaction. Journal of Materials Chemistry A, 2017, 5, 15552-15558.	10.3	81
165	Exciton Mapping at Subwavelength Scales in Two-Dimensional Materials. Physical Review Letters, 2015, 114, 107601.	7.8	79
166	Enhanced Electrocatalytic Activity of MoS _{<i>x</i>} on TCNQ-Treated Electrode for Hydrogen Evolution Reaction. ACS Applied Materials & Interfaces, 2014, 6, 17679-17685.	8.0	78
167	Scalable Approach To Construct Free-Standing and Flexible Carbon Networks for Lithium–Sulfur Battery. ACS Applied Materials & Interfaces, 2017, 9, 8047-8054.	8.0	78
168	High quantity and quality few-layers transition metal disulfide nanosheets from wet-milling exfoliation. RSC Advances, 2013, 3, 13193.	3.6	76
169	Functional Two-Dimensional Coordination Polymeric Layer as a Charge Barrier in Li–S Batteries. ACS Nano, 2018, 12, 836-843.	14.6	76
170	Band Alignment of 2D Transition Metal Dichalcogenide Heterojunctions. Advanced Functional Materials, 2017, 27, 1603756.	14.9	74
171	Charge Dynamics and Electronic Structures of Monolayer MoS ₂ Films Grown by Chemical Vapor Deposition. Applied Physics Express, 2013, 6, 125801.	2.4	73
172	Pressure-Induced Single-Walled Carbon Nanotube (<i>n,m</i>) Selectivity on Coâ^'Mo Catalysts. Journal of Physical Chemistry C, 2007, 111, 14612-14616.	3.1	72
173	Growth selectivity of hexagonal-boron nitride layers on Ni with various crystal orientations. RSC Advances, 2012, 2, 111-115.	3.6	72
174	Band Alignment at GaN/Single-Layer WSe ₂ Interface. ACS Applied Materials & Interfaces, 2017, 9, 9110-9117.	8.0	72
175	Enhanced thermoelectric power in two-dimensional transition metal dichalcogenide monolayers. Physical Review B, 2016, 94, .	3.2	71
176	Chemically modified graphene: flame retardant or fuel for combustion?. Journal of Materials Chemistry, 2011, 21, 3277-3279.	6.7	70
177	Dynamical observations on the crack tip zone and stress corrosion of two-dimensional MoS2. Nature Communications, 2017, 8, 14116.	12.8	69
178	Review—Two-Dimensional Layered Materials for Energy Storage Applications. ECS Journal of Solid State Science and Technology, 2016, 5, Q3021-Q3025.	1.8	68
179	Optoelectronic Ferroelectric Domainâ€Wall Memories Made from a Single Van Der Waals Ferroelectric. Advanced Functional Materials, 2020, 30, 2004206.	14.9	67
180	Degradable Conjugated Polymers: Synthesis and Applications in Enrichment of Semiconducting Singleâ€Walled Carbon Nanotubes. Advanced Functional Materials, 2011, 21, 1643-1651.	14.9	66

#	Article	IF	CITATIONS
181	Toward High-Performance Solution-Processed Carbon Nanotube Network Transistors by Removing Nanotube Bundles. Journal of Physical Chemistry C, 2008, 112, 12089-12091.	3.1	64
182	Determination of band offsets at GaN/single-layer MoS2 heterojunction. Applied Physics Letters, 2016, 109, .	3.3	64
183	Phase Inversion Strategy to Flexible Freestanding Electrode: Critical Coupling of Binders and Electrolytes for High Performance Li–S Battery. Advanced Functional Materials, 2018, 28, 1802244.	14.9	64
184	Layer-Dependent and In-Plane Anisotropic Properties of Low-Temperature Synthesized Few-Layer PdSe ₂ Single Crystals. ACS Nano, 2020, 14, 4963-4972.	14.6	64
185	Mixed-state electron ptychography enables sub-angstrom resolution imaging with picometer precision at low dose. Nature Communications, 2020, 11, 2994.	12.8	63
186	Giant Ferroelectric Resistance Switching Controlled by a Modulatory Terminal for Lowâ€Power Neuromorphic Inâ€Memory Computing. Advanced Materials, 2021, 33, e2008709.	21.0	63
187	Label-free detection of ATP release from living astrocytes with high temporal resolution using carbon nanotube network. Biosensors and Bioelectronics, 2009, 24, 2716-2720.	10.1	62
188	Ultrathin 1T-phase MoS 2 nanosheets decorated hollow carbon microspheres as highly efficient catalysts for solar energy harvesting and storage. Journal of Power Sources, 2017, 345, 156-164.	7.8	62
189	Yield, variability, reliability, and stability of two-dimensional materials based solid-state electronic devices. Nature Communications, 2020, 11, 5689.	12.8	62
190	Quasi-Two-Dimensional Se-Terminated Bismuth Oxychalcogenide (Bi ₂ O ₂ Se). ACS Nano, 2019, 13, 13439-13444.	14.6	61
191	Effect of different catalyst supports on the (n,m) selective growth of single-walled carbon nanotube from Co–Mo catalyst. Journal of Materials Science, 2009, 44, 3285-3295.	3.7	60
192	Hall effect biosensors with ultraclean graphene film for improved sensitivity of label-free DNA detection. Biosensors and Bioelectronics, 2018, 99, 85-91.	10.1	60
193	Chirality Assignment of Single-Walled Carbon Nanotubes with Strain. Physical Review Letters, 2004, 93, 156104.	7.8	59
194	Evolution of magnetostructural transition and magnetocaloric effect with Al doping in MnCoGe _{1â^'<i>x</i>} Al _{<i>x</i>} compounds. Journal Physics D: Applied Physics, 2014, 47, 055003.	2.8	59
195	One‣tep Formation of a Single Atomic‣ayer Transistor by the Selective Fluorination of a Graphene Film. Small, 2014, 10, 989-997.	10.0	59
196	Synthesis and characterization of one-dimensional CdSe by a novel reverse micelle assisted hydrothermal method. Journal of Colloid and Interface Science, 2008, 320, 491-500.	9.4	58
197	Electronic Properties of a 1D Intrinsic/p-Doped Heterojunction in a 2D Transition Metal Dichalcogenide Semiconductor. ACS Nano, 2017, 11, 9128-9135.	14.6	58
198	Selective Enrichment of (6,5) and (8,3) Single-Walled Carbon Nanotubes via Cosurfactant Extraction from Narrow (<i>n</i> , <i>m</i>) Distribution Samples. Journal of Physical Chemistry B, 2008, 112, 2771-2774.	2.6	57

#	Article	IF	CITATIONS
199	Flexible transparent electrodes made of electrochemically exfoliated graphene sheets from low-cost graphite pieces. Displays, 2013, 34, 315-319.	3.7	56
200	Flexible and stretchable thin-film transistors based on molybdenum disulphide. Physical Chemistry Chemical Physics, 2014, 16, 14996.	2.8	56
201	Tailoring excitonic states of van der Waals bilayers through stacking configuration, band alignment, and valley spin. Science Advances, 2019, 5, eaax7407.	10.3	56
202	Direct conversion of multilayer molybdenum trioxide to nanorods as multifunctional electrodes in lithium-ion batteries. Nanoscale, 2014, 6, 5484-5490.	5.6	55
203	Gap States at Low-Angle Grain Boundaries in Monolayer Tungsten Diselenide. Nano Letters, 2016, 16, 3682-3688.	9.1	55
204	Oxygen Passivation Mediated Tunability of Trion and Excitons in <mml:math xmlns:mml="http://www.w3.org/1998/Math/MathML" display="inline"><mml:mrow><mml:msub><mml:mrow><mml:mi>MoS</mml:mi></mml:mrow><ml:mrow><m Physical Review Letters, 2017, 119, 077402.</m </ml:mrow></mml:msub></mml:mrow></mml:math 	ml:mn>2<	:/m͡ml:mn>
205	Energy Transfer from Photo-Excited Fluorene Polymers to Single-Walled Carbon Nanotubes. Journal of Physical Chemistry C, 2009, 113, 14946-14952.	3.1	54
206	Facile synthesis of carbon/MoO 3 nanocomposites as stable battery anodes. Journal of Power Sources, 2017, 348, 270-280.	7.8	54
207	The effects of nitrogen and boron doping on the optical emission and diameters of single-walled carbon nanotubes. Carbon, 2006, 44, 2752-2757.	10.3	53
208	Near-field Raman imaging using optically trapped dielectric microsphere. Optics Express, 2008, 16, 7976.	3.4	52
209	High-Current Gain Two-Dimensional MoS ₂ -Base Hot-Electron Transistors. Nano Letters, 2015, 15, 7905-7912.	9.1	52
210	Laterally Stitched Heterostructures of Transition Metal Dichalcogenide: Chemical Vapor Deposition Growth on Lithographically Patterned Area. ACS Nano, 2016, 10, 10516-10523.	14.6	52
211	Temperature-dependent optical constants of monolayer \$\${ext {MoS}}_2\$\$, \$\${ext {MoSe}}_2\$\$, \$\${ext {WS}}_2\$\$, and \$\${ext {WSe}}_2\$\$: spectroscopic ellipsometry and first-principles calculations. Scientific Reports, 2020, 10, 15282.	3.3	52
212	Redox Species-Based Electrolytes for Advanced Rechargeable Lithium Ion Batteries. ACS Energy Letters, 2016, 1, 529-534.	17.4	51
213	Electrical detection of hybridization and threading intercalation of deoxyribonucleic acid using carbon nanotube network field-effect transistors. Applied Physics Letters, 2006, 89, 232104.	3.3	50
214	Solutionâ€Processable Carbon Nanotubes for Semiconducting Thinâ€Film Transistor Devices. Advanced Materials, 2010, 22, 1278-1282.	21.0	50
215	Unusual Activity of Rationally Designed Cobalt Phosphide/Oxide Heterostructure Composite for Hydrogen Production in Alkaline Medium. ACS Nano, 2022, 16, 3906-3916.	14.6	50
216	Comparative study of photoluminescence of single-walled carbon nanotubes wrapped with sodium dodecyl sulfate, surfactin and polyvinylpyrrolidone. Nanotechnology, 2005, 16, S202-S205.	2.6	49

#	Article	IF	CITATIONS
217	Plasma-assisted electrochemical exfoliation of graphite for rapid production of graphene sheets. RSC Advances, 2014, 4, 6946.	3.6	49
218	Two-dimensional materials as anodes for sodium-ion batteries. Materials Today Advances, 2020, 6, 100054.	5.2	49
219	Two-Dimensional Cs ₂ AgBiBr ₆ /WS ₂ Heterostructure-Based Photodetector with Boosted Detectivity via Interfacial Engineering. ACS Nano, 2022, 16, 3985-3993.	14.6	49
220	Selfâ€Aligned and Scalable Growth of Monolayer WSe ₂ –MoS ₂ Lateral Heterojunctions. Advanced Functional Materials, 2018, 28, 1706860.	14.9	48
221	Electrical detection of nitric oxide using single-walled carbon nanotube network devices. Carbon, 2007, 45, 1911-1914.	10.3	46
222	Integrating carbon nanotubes and lipid bilayer for biosensing. Biosensors and Bioelectronics, 2010, 25, 1834-1837.	10.1	46
223	Flexible Electrochromic Devices Based on Optoelectronically Active Polynorbornene Layer and Ultratransparent Graphene Electrodes. Macromolecules, 2011, 44, 9550-9555.	4.8	46
224	Characteristics of a sensitive micro-Hall probe fabricated on chemical vapor deposited graphene over the temperature range from liquid-helium to room temperature. Applied Physics Letters, 2011, 99, .	3.3	45
225	The electrical properties of graphene modified by bromophenyl groups derived from a diazonium compound. Carbon, 2012, 50, 1517-1522.	10.3	45
226	Controlled mechanical cleavage of bulk niobium diselenide to nanoscaled sheet, rod, and particle structures for Pt-free dye-sensitized solar cells. Journal of Materials Chemistry A, 2014, 2, 11382-11390.	10.3	45
227	Pressureâ€Induced Charge Transfer Doping of Monolayer Graphene/MoS ₂ Heterostructure. Small, 2016, 12, 4063-4069.	10.0	45
228	Atomic-Monolayer Two-Dimensional Lateral Quasi-Heterojunction Bipolar Transistors with Resonant Tunneling Phenomenon. ACS Nano, 2017, 11, 11015-11023.	14.6	45
229	Analysis of flavonoids by graphene-based surface-assisted laser desorption/ionization time-of-flight mass spectrometry. Analyst, The, 2012, 137, 5809.	3.5	44
230	Nitrogenâ€Doped Carbon Nanotubeâ€Based Bilayer Thin Film as Transparent Counter Electrode for Dyeâ€Sensitized Solar Cells (DSSCs). Chemistry - an Asian Journal, 2012, 7, 541-545.	3.3	44
231	Dielectric impact on exciton binding energy and quasiparticle bandgap in monolayer WS ₂ and WSe ₂ . 2D Materials, 2019, 6, 025028.	4.4	44
232	Synthesis and structure of two-dimensional transition-metal dichalcogenides. MRS Bulletin, 2015, 40, 566-576.	3.5	43
233	Ultrasensitive Detection of DNA Molecules with High On/Off Singleâ€Walled Carbon Nanotube Network. Advanced Materials, 2010, 22, 4867-4871.	21.0	42
234	Unraveling Spatially Heterogeneous Ultrafast Carrier Dynamics of Single-Layer WSe ₂ by Femtosecond Time-Resolved Photoemission Electron Microscopy. Nano Letters, 2018, 18, 5172-5178.	9.1	42

#	Article	IF	CITATIONS
235	Toward the Growth of High Mobility 2D Transition Metal Dichalcogenide Semiconductors. Advanced Materials Interfaces, 2019, 6, 1900220.	3.7	42
236	Atomic-Monolayer MoS ₂ Band-to-Band Tunneling Field-Effect Transistor. Small, 2016, 12, 5676-5683.	10.0	41
237	Enhancing the electrocatalytic water splitting efficiency for amorphous MoS. International Journal of Hydrogen Energy, 2014, 39, 4788-4793.	7.1	40
238	Trilayered MoS\$_{f 2}\$ Metal –Semiconductor–Metal Photodetectors: Photogain and Radiation Resistance. IEEE Journal of Selected Topics in Quantum Electronics, 2014, 20, 30-35.	2.9	40
239	Resonant Tunneling through Discrete Quantum States in Stacked Atomic-Layered MoS2. Nano Letters, 2014, 14, 2381-2386.	9.1	40
240	Efficient electrochemical transformation of CO ₂ to C ₂ /C ₃ chemicals on benzimidazole-functionalized copper surfaces. Chemical Communications, 2018, 54, 11324-11327.	4.1	39
241	Power Factor Enhancement for Few-Layered Graphene Films by Molecular Attachments. Journal of Physical Chemistry C, 2011, 115, 1780-1785.	3.1	38
242	Terahertz optical properties of multilayer graphene: Experimental observation of strong dependence on stacking arrangements and misorientation angles. Physical Review B, 2012, 86, .	3.2	38
243	Electrical Probing of Submicroliter Liquid Using Graphene Strip Transistors Built on a Nanopipette. Small, 2012, 8, 43-46.	10.0	38
244	Impact of N-plasma and Ga-irradiation on MoS2 layer in molecular beam epitaxy. Applied Physics Letters, 2017, 110, .	3.3	38
245	Demonstration of the key substrate-dependent charge transfer mechanisms between monolayer MoS2 and molecular dopants. Communications Physics, 2019, 2, .	5.3	38
246	Continuous desalination with a metal-free redox-mediator. Journal of Materials Chemistry A, 2019, 7, 13941-13947.	10.3	38
247	High On-State Current in Chemical Vapor Deposited Monolayer MoS ₂ nFETs With Sn Ohmic Contacts. IEEE Electron Device Letters, 2021, 42, 272-275.	3.9	38
248	Label-Free Electronic Detection of DNA Using Simple Double-Walled Carbon Nanotube Resistors. Journal of Physical Chemistry C, 2008, 112, 9891-9895.	3.1	37
249	A Versatile and Simple Approach to Generate Light Emission in Semiconductors Mediated by Electric Double Layers. Advanced Materials, 2017, 29, 1606918.	21.0	37
250	Low-defect-density WS2 by hydroxide vapor phase deposition. Nature Communications, 2022, 13, .	12.8	37
251	Anomalous lattice vibrations of monolayer MoS ₂ probed by ultraviolet Raman scattering. Physical Chemistry Chemical Physics, 2015, 17, 14561-14568.	2.8	36
252	Metalâ€Guided Selective Growth of 2D Materials: Demonstration of a Bottomâ€Up CMOS Inverter. Advanced Materials, 2019, 31, e1900861.	21.0	36

#	Article	IF	CITATIONS
253	Engineering Point-Defect States in Monolayer WSe ₂ . ACS Nano, 2019, 13, 1595-1602.	14.6	35
254	Molecular adsorption induces the transformation of rhombohedral- to Bernal-stacking order in trilayer graphene. Nature Communications, 2013, 4, 2074.	12.8	34
255	Ultrafast Multi-Level Logic Gates with Spin-Valley Coupled Polarization Anisotropy in Monolayer MoS2. Scientific Reports, 2015, 5, 8289.	3.3	34
256	Green Strategy to Single Crystalline Anatase TiO ₂ Nanosheets with Dominant (001) Facets and Its Lithiation Study toward Sustainable Cobalt-Free Lithium Ion Full Battery. ACS Sustainable Chemistry and Engineering, 2015, 3, 3086-3095.	6.7	34
257	Graphite edge controlled registration of monolayer MoS2 crystal orientation. Applied Physics Letters, 2015, 106, 181904.	3.3	34
258	Large-area few-layer MoS ₂ deposited by sputtering. Materials Research Express, 2016, 3, 065007.	1.6	34
259	Plasmonicâ€Enhanced Light Harvesting and Perovskite Solar Cell Performance Using Au Biometric Dimers with Broadband Structural Darkness. Solar Rrl, 2019, 3, 1900138.	5.8	34
260	Chirality-dependent boron-mediated growth of nitrogen-doped single-walled carbon nanotubes. Physical Review B, 2005, 72, .	3.2	33
261	Crystal-encapsulation-induced band-structure change in single-walled carbon nanotubes: Photoluminescence and Raman spectra. Physical Review B, 2006, 74, .	3.2	33
262	Solution-processable semiconducting thin-film transistors using single-walled carbon nanotubes chemically modified by organic radical initiators. Chemical Communications, 2009, , 7182.	4.1	33
263	Label-free electrical detection of DNA hybridization using carbon nanotubes and graphene. Nano Reviews, 2010, 1, 5354.	3.7	33
264	Ultra-low-edge-defect graphene nanoribbons patterned by neutral beam. Carbon, 2013, 61, 229-235.	10.3	33
265	InGaN/GaN nanowires epitaxy on large-area MoS2 for high-performance light-emitters. RSC Advances, 2017, 7, 26665-26672.	3.6	32
266	Enhanced Emission from WSe ₂ Monolayers Coupled to Circular Bragg Gratings. ACS Photonics, 2018, 5, 3950-3955.	6.6	31
267	Scalable fabrication of a complementary logic inverter based on MoS ₂ fin-shaped field effect transistors. Nanoscale Horizons, 2019, 4, 683-688.	8.0	31
268	Work function engineering of electrodes via electropolymerization of ethylenedioxythiophenes and its derivatives. Organic Electronics, 2008, 9, 859-863.	2.6	30
269	Type-I band alignment at MoS2/In0.15Al0.85N lattice matched heterojunction and realization of MoS2 quantum well. Applied Physics Letters, 2017, 111, .	3.3	30
270	Nanoscale Surface Photovoltage Mapping of 2D Materials and Heterostructures by Illuminated Kelvin Probe Force Microscopy. Journal of Physical Chemistry C, 2018, 122, 13564-13571.	3.1	30

#	Article	IF	CITATIONS
271	Solution-Processed Mixed-Dimensional Hybrid Perovskite/Carbon Nanotube Electronics. ACS Nano, 2020, 14, 3969-3979.	14.6	30
272	Origin of hysteresis in the transfer characteristic of carbon nanotube field effect transistor. Journal Physics D: Applied Physics, 2011, 44, 285301.	2.8	29
273	Efficient Heat Dissipation of Photonic Crystal Microcavity by Monolayer Graphene. ACS Nano, 2013, 7, 10818-10824.	14.6	29
274	Transmissive-to-black fast electrochromic switching from a long conjugated pendant group and a highly dispersed polymer/SWNT. Polymer Chemistry, 2018, 9, 619-626.	3.9	29
275	Van der Waals heterostructures with one-dimensional atomic crystals. Progress in Materials Science, 2021, 122, 100856.	32.8	29
276	Transfer printing of graphene strip from the graphene grown on copper wires. Nanotechnology, 2011, 22, 185309.	2.6	28
277	A facile approach to nanoarchitectured three-dimensional graphene-based Li–Mn–O composite as high-power cathodes for Li-ion batteries. Beilstein Journal of Nanotechnology, 2012, 3, 513-523.	2.8	28
278	Deep-ultraviolet Raman scattering studies of monolayer graphene thin films. Carbon, 2015, 81, 807-813.	10.3	28
279	Magnetic separation of Fe catalyst from single-walled carbon nanotubes in an aqueous surfactant solution. Carbon, 2005, 43, 1151-1155.	10.3	27
280	Enrichment of (8,4) Singleâ€Walled Carbon Nanotubes Through Coextraction with Heparin. Small, 2010, 6, 110-118.	10.0	27
281	Atomic-Layer Controlled Interfacial Band Engineering at Two-Dimensional Layered PtSe ₂ /Si Heterojunctions for Efficient Photoelectrochemical Hydrogen Production. ACS Nano, 2021, 15, 4627-4635.	14.6	27
282	Poly(3,3‴-didodecylquarterthiophene) field effect transistors with single-walled carbon nanotube based source and drain electrodes. Applied Physics Letters, 2007, 91, 223512.	3.3	26
283	Effect of Centrifugation on the Purity of Single-Walled Carbon Nanotubes from MCM-41 Containing Cobalt. Journal of Physical Chemistry C, 2008, 112, 17567-17575.	3.1	26
284	Graphene-Au nanoparticle based vertical heterostructures: A novel route towards high- ZT Thermoelectric devices. Nano Energy, 2017, 38, 385-391.	16.0	26
285	Energy-Resolved Photoconductivity Mapping in a Monolayer–Bilayer WSe2 Lateral Heterostructure. Nano Letters, 2018, 18, 7200-7206.	9.1	26
286	Metal contact and carrier transport in single crystalline CH3NH3PbBr3 perovskite. Nano Energy, 2018, 53, 817-827.	16.0	26
287	Steam-Assisted Chemical Vapor Deposition of Zeolitic Imidazolate Framework. , 2020, 2, 485-491.		26
288	Unraveling the origin of ferroelectric resistance switching through the interfacial engineering of layered ferroelectric-metal junctions. Nature Communications, 2021, 12, 7291.	12.8	26

#	Article	IF	CITATIONS
289	Label-free detection of alanine aminotransferase using a graphene field-effect biosensor. Sensors and Actuators B: Chemical, 2013, 182, 396-400.	7.8	25
290	TMD FinFET with 4 nm thin body and back gate control for future low power technology. , 2015, , .		25
291	Circular Dichroism Control of Tungsten Diselenide (WSe ₂) Atomic Layers with Plasmonic Metamolecules. ACS Applied Materials & Interfaces, 2018, 10, 15996-16004.	8.0	25
292	Recent Advances in van der Waals Heterojunctions Based on Semiconducting Transition Metal Dichalcogenides. Advanced Electronic Materials, 2018, 4, 1800270.	5.1	25
293	Layer Rotation-Angle-Dependent Excitonic Absorption in van der Waals Heterostructures Revealed by Electron Energy Loss Spectroscopy. ACS Nano, 2019, 13, 9541-9550.	14.6	25
294	One-Step Vapor-Phase Synthesis and Quantum-Confined Exciton in Single-Crystal Platelets of Hybrid Halide Perovskites. Journal of Physical Chemistry Letters, 2019, 10, 2363-2371.	4.6	25
295	The Schottky–Mott Rule Expanded for Two-Dimensional Semiconductors: Influence of Substrate Dielectric Screening. ACS Nano, 2021, 15, 14794-14803.	14.6	25
296	Physical and Barrier Properties of Amorphous Silicon-Oxycarbide Deposited by PECVD from Octamethylcyclotetrasiloxane. Journal of the Electrochemical Society, 2004, 151, G612.	2.9	24
297	Photoresponse in Self-Assembled Films of Carbon Nanotubes. Journal of Physical Chemistry C, 2008, 112, 13004-13009.	3.1	24
298	Nanotopographic Carbon Nanotube Thinâ€Film Substrate Freezes Lateral Motion of Secretory Vesicles. Advanced Materials, 2009, 21, 790-793.	21.0	24
299	Novel poly(triphenylamine- <i>alt</i> -fluorene) with asymmetric hexaphenylbenzene and pyrene moieties: synthesis, fluorescence, flexible near-infrared electrochromic devices and theoretical investigation. Polymer Chemistry, 2016, 7, 1505-1516.	3.9	24
300	MoS _x -coated NbS ₂ nanoflakes grown on glass carbon: an advanced electrocatalyst for the hydrogen evolution reaction. Nanoscale, 2018, 10, 3444-3450.	5.6	24
301	Tuning of electrical characteristics in networked carbon nanotube field-effect transistors using thiolated molecules. Applied Physics Letters, 2007, 91, 103515.	3.3	23
302	Effect of different carbon sources on the growth of single-walled carbon nanotube from MCM-41 containing nickel. Carbon, 2007, 45, 2217-2228.	10.3	23
303	Charge injection at carbon nanotube-SiO2 interface. Applied Physics Letters, 2008, 93, 093509.	3.3	23
304	High-performance graphene/sulphur electrodes for flexible Li-ion batteries using the low-temperature spraying method. Nanoscale, 2015, 7, 8093-8100.	5.6	23
305	Scalable Patterning of MoS ₂ Nanoribbons by Micromolding in Capillaries. ACS Applied Materials & Materia	8.0	23
306	Magneto-optical studies of single-wall carbon nanotubes. Physical Review B, 2007, 76, .	3.2	22

#	Article	IF	CITATIONS
307	Flipping nanoscale ripples of free-standing graphene using a scanning tunneling microscope tip. Carbon, 2014, 77, 236-243.	10.3	22
308	Integration of ammonia-plasma-functionalized graphene nanodiscs as charge trapping centers for nonvolatile memory applications. Carbon, 2017, 113, 318-324.	10.3	22
309	First demonstration of 40-nm channel length top-gate WS ₂ pFET using channel area-selective CVD growth directly on SiO _x /Si substrate. , 2019, , .		22
310	Mobility-Fluctuation-Controlled Linear Positive Magnetoresistance in 2D Semiconductor Bi ₂ O ₂ Se Nanoplates. ACS Nano, 2020, 14, 11319-11326.	14.6	22
311	Electrocatalytic Reduction of Carbon Dioxide with a Wellâ€Defined PN ³ â^'Ru Pincer Complex. ChemPlusChem, 2016, 81, 166-171.	2.8	21
312	High-efficiency omnidirectional photoresponses based on monolayer lateral p–n heterojunctions. Nanoscale Horizons, 2017, 2, 37-42.	8.0	21
313	Electrochemical Conversion of CO ₂ to 2-Bromoethanol in a Membraneless Cell. ACS Energy Letters, 2019, 4, 600-605.	17.4	21
314	Bulk Crystallization Behavior of Poly(Îμ-caprolactone) with a Wide Range of Molecular Weight. Polymer Journal, 1997, 29, 889-893.	2.7	20
315	Ultrafast dynamics of hot electrons and phonons in chemical vapor deposited graphene. Journal of Applied Physics, 2013, 113, 133511.	2.5	20
316	Growth of 2H stacked WSe ₂ bilayers on sapphire. Nanoscale Horizons, 2019, 4, 1434-1442.	8.0	20
317	Design and Mechanistic Study of Highly Durable Carbon-Coated Cobalt Diphosphide Core–Shell Nanostructure Electrocatalysts for the Efficient and Stable Oxygen Evolution Reaction. ACS Applied Materials & Interfaces, 2019, 11, 20752-20761.	8.0	20
318	Graphene-GaAs/AlxGa1â^'xAs heterostructure dual-function field-effect transistor. Applied Physics Letters, 2012, 101, .	3.3	19
319	An Aqueous Rechargeable Fluoride Ion Battery with Dual Fluoride Electrodes. Journal of the Electrochemical Society, 2019, 166, A2419-A2424.	2.9	19
320	Typeâ€I Energy Level Alignment at the PTCDA—Monolayer MoS ₂ Interface Promotes Resonance Energy Transfer and Luminescence Enhancement. Advanced Science, 2021, 8, 2100215.	11.2	19
321	Facile Doping in Two-Dimensional Transition-Metal Dichalcogenides by UV Light. ACS Applied Materials & Interfaces, 2018, 10, 29893-29901.	8.0	18
322	Wafer-scale single-orientation 2D layers by atomic edge-guided epitaxial growth. Chemical Society Reviews, 2022, 51, 803-811.	38.1	18
323	Bi ₂ O ₂ Se-Based True Random Number Generator for Security Applications. ACS Nano, 2022, 16, 6847-6857.	14.6	18
324	Electropolymerization of pyrrole and 4-(3-Pyrrolyl)butane-sulfonate on Pt substrate: An in situ EQCM study. Thin Solid Films, 1997, 301, 175-182.	1.8	17

#	Article	IF	CITATIONS
325	Effects of O2- and N2-Plasma Treatments on Copper Surface. Japanese Journal of Applied Physics, 2004, 43, 7415-7418.	1.5	17
326	Photoconductivity from Carbon Nanotube Transistors Activated by Photosensitive Polymers. Journal of Physical Chemistry C, 2008, 112, 18201-18206.	3.1	17
327	Assessment of (n,m) Selectively Enriched Small Diameter Single-Walled Carbon Nanotubes by Density Differentiation from Cobalt-Incorporated MCM-41 for Macroelectronics. Chemistry of Materials, 2008, 20, 7417-7424.	6.7	17
328	Disorder-dependent valley properties in monolayer <mml:math xmlns:mml="http://www.w3.org/1998/Math/MathML"><mml:mrow><mml:mi>WS</mml:mi><mml:msub><mml:m mathvariant="normal">e<mml:mn>2</mml:mn></mml:m </mml:msub></mml:mrow>. Physical Review B, 2017, 96, .</mml:math 	ni 3.2	17
329	<i>In Operando</i> X-ray Studies of High-Performance Lithium-Ion Storage in Keplerate-Type Polyoxometalate Anodes. ACS Applied Materials & Interfaces, 2020, 12, 40296-40309.	8.0	17
330	Self-Exfoliated Synthesis of Transition Metal Phosphate Nanolayers for Selective Aerobic Oxidation of Ethyl Lactate to Ethyl Pyruvate. ACS Catalysis, 2020, 10, 3958-3967.	11.2	17
331	Heme-Enabled Electrical Detection of Carbon Monoxide at Room Temperature Using Networked Carbon Nanotube Field-Effect Transistors. Chemistry of Materials, 2007, 19, 6059-6061.	6.7	16
332	Charged impurity-induced scatterings in chemical vapor deposited graphene. Journal of Applied Physics, 2013, 114, 233703.	2.5	16
333	Bi ₂ O ₂ Se-Based Memristor-Aided Logic. ACS Applied Materials & Interfaces, 2021, 13, 15391-15398.	8.0	16
334	Bandgap-selective chemical doping of semiconducting single-walled carbon nanotubes. Nanotechnology, 2004, 15, 1844-1847.	2.6	15
335	Species-Dependent Energy Transfer of Surfactant-Dispersed Semiconducting Single-Walled Carbon Nanotubes. Journal of Physical Chemistry C, 2009, 113, 20061-20065.	3.1	15
336	Mobility Enhancement in Carbon Nanotube Transistors by Screening Charge Impurity with Silica Nanoparticles. Journal of Physical Chemistry C, 2011, 115, 6975-6979.	3.1	15
337	Photodetection in p–n junctions formed by electrolyte-gated transistors of two-dimensional crystals. Applied Physics Letters, 2016, 109, .	3.3	15
338	Synthesis and optoelectronic applications of graphene/transition metal dichalcogenides flat-pack assembly. Carbon, 2018, 127, 602-610.	10.3	15
339	Deep-ultraviolet Raman scattering spectroscopy of monolayer WS2. Scientific Reports, 2018, 8, 11398.	3.3	15
340	TDDB Reliability Improvement of Cu Damascene with a Bilayer-Structured α-SiC:H Dielectric Barrier. Journal of the Electrochemical Society, 2004, 151, G89.	2.9	14
341	Diameter―and Metallicityâ€5elective Enrichment of Singleâ€Walled Carbon Nanotubes Using Polymethacrylates with Pendant Aromatic Functional Groups. Small, 2010, 6, 1311-1320.	10.0	14
342	Sorting of Single-Walled Carbon Nanotubes Based on Metallicity by Selective Precipitation with Polyvinylpyrrolidone. Journal of Physical Chemistry C, 2011, 115, 5199-5206.	3.1	14

#	Article	IF	CITATIONS
343	Plasma electrolysis allows the facile and efficient production of graphite oxide from recycled graphite. RSC Advances, 2013, 3, 17402.	3.6	14
344	Polymerâ€Free Patterning of Graphene at Subâ€10â€nm Scale by Lowâ€Energy Repetitive Electron Beam. Small, 2014, 10, 4778-4784.	10.0	14
345	Optical properties of nitrogen-doped graphene thin films probed by spectroscopic ellipsometry. Thin Solid Films, 2014, 571, 675-679.	1.8	14
346	Electron energy loss spectroscopy of excitons in two-dimensional-semiconductors as a function of temperature. Applied Physics Letters, 2016, 108, .	3.3	14
347	Anomalous photoluminescence thermal quenching of sandwiched single layer MoS_2. Optical Materials Express, 2017, 7, 3697.	3.0	14
348	Negative capacitance from the inductance of ferroelectric switching. Communications Physics, 2019, 2, .	5.3	14
349	Phase behaviours of diphenylsiloxane oligomers. Polymer, 1998, 39, 689-695.	3.8	13
350	Properties of narrow gap quantum dots and wells in the InAs/InSb/GaSb systems. Physica E: Low-Dimensional Systems and Nanostructures, 2004, 20, 204-210.	2.7	13
351	The screening of charged impurities in bilayer graphene. New Journal of Physics, 2010, 12, 103037.	2.9	13
352	Selective Small-Diameter Metallic Single-Walled Carbon Nanotube Removal by Mere Standing with Anthraquinone and Application to a Field-Effect Transistor. Journal of Physical Chemistry C, 2010, 114, 21035-21041.	3.1	13
353	Observation of Phonon Anomaly at the Armchair Edge of Single-Layer Graphene in Air. ACS Nano, 2011, 5, 3347-3353.	14.6	13
354	Simultaneous functionalization and reduction of graphene oxide with diatom silica. Journal of Materials Science, 2013, 48, 3415-3421.	3.7	13
355	Moiré-related in-gap states in a twisted MoS2/graphite heterojunction. Npj 2D Materials and Applications, 2017, 1, .	7.9	13
356	A Nanostructuring Method to Decouple Electrical and Thermal Transport through the Formation of Electrically Triggered Conductive Nanofilaments. Advanced Materials, 2018, 30, e1705385.	21.0	13
357	Effective N-methyl-2-pyrrolidone wet cleaning for fabricating high-performance monolayer MoS2 transistors. Nano Research, 2019, 12, 303-308.	10.4	13
358	Aberration-corrected STEM imaging of 2D materials: Artifacts and practical applications of threefold astigmatism. Science Advances, 2020, 6, .	10.3	13
359	Capturing 3D atomic defects and phonon localization at the 2D heterostructure interface. Science Advances, 2021, 7, eabi6699.	10.3	13
360	Leakage mechanism in Cu damascene structure with methylsilane-doped low-K CVD oxide as intermetal dielectric. IEEE Electron Device Letters, 2001, 22, 263-265.	3.9	12

#	Article	IF	CITATIONS
361	Aggregation-Dependent Photoluminescence Sidebands in Single-Walled Carbon Nanotube. Journal of Physical Chemistry C, 2010, 114, 6704-6711.	3.1	12
362	Efficient reduction of graphene oxide catalyzed by copper. Physical Chemistry Chemical Physics, 2012, 14, 3083.	2.8	12
363	Hybrid Si/TMD 2D electronic double channels fabricated using solid CVD few-layer-MoS2 stacking for V <inf>th</inf> matching and CMOS-compatible 3DFETs. , 2014, , .		12
364	Dirac fermion relaxation and energy loss rate near the Fermi surface in monolayer and multilayer graphene. Nanoscale, 2014, 6, 8575-8578.	5.6	12
365	Dual-mode operation of 2D material-base hot electron transistors. Scientific Reports, 2016, 6, 32503.	3.3	12
366	Ultrasensitive broadband photodetectors based on two-dimensional Bi ₂ O ₂ Te films. Journal of Materials Chemistry C, 2021, 9, 13713-13721.	5.5	12
367	Temperatureâ€Dependent Electronic Groundâ€State Charge Transfer in van der Waals Heterostructures. Advanced Materials, 2021, 33, e2008677.	21.0	12
368	2D Materialsâ€Based Static Randomâ€Access Memory. Advanced Materials, 2022, 34, e2107894.	21.0	12
369	N-type behavior of ferroelectric-gate carbon nanotube network transistor. Applied Physics Letters, 2008, 93, 082103.	3.3	11
370	Low-Cost and Ultra-Strong p-Type Doping of Carbon Nanotube Films by a Piranha Mixture. European Journal of Inorganic Chemistry, 2011, 2011, 4182-4186.	2.0	11
371	Seeing Twoâ€Dimensional Sheets on Arbitrary Substrates by Fluorescence Quenching Microscopy. Small, 2013, 9, 3253-3258.	10.0	11
372	Few layer graphene paper from electrochemical process for heat conduction. Materials Research Innovations, 2014, 18, 208-213.	2.3	11
373	Advances in Twoâ€Ðimensional Layered Materials. Advanced Functional Materials, 2017, 27, 1701403.	14.9	11
374	Electronic band dispersion determination in azimuthally disordered transition-metal dichalcogenide monolayers. Communications Physics, 2019, 2, .	5.3	11
375	Energy-Efficient Monolithic 3-D SRAM Cell With BEOL MoS2 FETs for SoC Scaling. IEEE Transactions on Electron Devices, 2020, 67, 4216-4221.	3.0	11
376	Optically Controlled Ferroelectric Nanodomains for Logic-in-Memory Photonic Devices With Simplified Structures. IEEE Transactions on Electron Devices, 2021, 68, 1992-1995.	3.0	11
377	MAGNETO-PHOTOLUMINESCENCE OF CHIRALITY-CHARACTERIZED SINGLE-WALLED CARBON NANOTUBES. International Journal of Modern Physics B, 2004, 18, 3509-3512.	2.0	10
378	Large-area WSe ₂ electric double layer transistors on a plastic substrate. Japanese Journal of Applied Physics, 2015, 54, 06FF06.	1.5	10

#	Article	IF	CITATIONS
379	MoS <inf>2</inf> U-shape MOSFET with 10 nm channel length and poly-Si source/drain serving as seed for full wafer CVD MoS <inf>2</inf> availability. , 2016, , .		10
380	Editors' Choice—Growth of Layered WS ₂ Electrocatalysts for Highly Efficient Hydrogen Production Reaction. ECS Journal of Solid State Science and Technology, 2016, 5, Q3067-Q3071.	1.8	10
381	Cross-plane thermoelectric figure of merit in graphene - C60 heterostructures at room temperature. FlatChem, 2019, 14, 100089.	5.6	10
382	Effects of substrates on photocurrents from photosensitive polymer coated carbon nanotube networks. Applied Physics Letters, 2008, 92, .	3.3	9
383	Charge dynamics and electronic structures of monolayer graphene with molecular doping. Applied Physics Letters, 2012, 101, 111907.	3.3	9
384	Effects of electrolyte gating on photoluminescence spectra of large-area WSe2monolayer films. Japanese Journal of Applied Physics, 2016, 55, 06GB02.	1.5	9
385	Chemical hole doping into large-area transition metal dichalcogenide monolayers using boron-based oxidant. Japanese Journal of Applied Physics, 2018, 57, 02CB15.	1.5	9
386	Epitaxial Growth and Determination of Band Alignment of Bi ₂ Te ₃ –WSe ₂ Vertical van der Waals Heterojunctions. , 2020, 2, 1351-1359.		9
387	Strain-Directed Layer-By-Layer Epitaxy Toward van der Waals Homo- and Heterostructures. , 2021, 3, 442-453.		9
388	Synthesis and properties of novel aromatic polyimides derived from bis(p-aminophenoxy)methylphenylsilane. Journal of Applied Polymer Science, 1997, 63, 369-376.	2.6	8
389	Highly Efficient Electrocatalytic Hydrogen Production by MoS <i>_x</i> Grown on Grapheneâ€Protected 3D Ni Foams (Adv. Mater. 5/2013). Advanced Materials, 2013, 25, 755-755.	21.0	8
390	Efficiency Enhancement of InGaN-Based Solar Cells via Stacking Layers of Light-Harvesting Nanospheres. Scientific Reports, 2016, 6, 28671.	3.3	8
391	Surface-reconstructed Cu electrode via a facile electrochemical anodization-reduction process for low overpotential CO2 reduction. Journal of Saudi Chemical Society, 2017, 21, 708-712.	5.2	8
392	Spatial Control of Dynamic <i>p–i–n</i> Junctions in Transition Metal Dichalcogenide Light-Emitting Devices. ACS Nano, 2021, 15, 12911-12921.	14.6	8
393	Pinning-Free Edge Contact Monolayer MoS ₂ FET. , 2020, , .		8
394	Illumination-Enhanced Hysteresis of Transistors Based on Carbon Nanotube Networks. Journal of Physical Chemistry C, 2009, 113, 4745-4747.	3.1	7
395	Direct Intermolecular Force Measurements between Functional Groups and Individual Metallic or Semiconducting Singleâ€Walled Carbon Nanotubes. Small, 2014, 10, 750-757.	10.0	7
396	Liquid-solid surface phase transformation of fluorinated fullerene on monolayer tungsten diselenide. Physical Review B, 2018, 97, .	3.2	7

#	Article	IF	CITATIONS
397	Two-dimensional solid-phase crystallization toward centimeter-scale monocrystalline layered MoTe ₂ <i>via</i> two-step annealing. Journal of Materials Chemistry C, 2021, 9, 15566-15576.	5.5	7
398	Scalable nanoimprint patterning of thin graphitic oxide sheets and <i>in situ</i> reduction. Journal of Vacuum Science and Technology B:Nanotechnology and Microelectronics, 2011, 29, 011023.	1.2	6
399	Atomic Layer Nucleation Engineering: Inhibitor-Free Area-Selective Atomic Layer Deposition of Oxide and Nitride. Chemistry of Materials, 2021, 33, 5584-5590.	6.7	6
400	Bottom-Up Synthesized All-Thermal-Catalyst Aerogels for Heat-Regenerative Air Filtration. Nano Letters, 2021, 21, 8160-8165.	9.1	6
401	<i>IN SITU</i> FORMATION OF COBALT NANOCLUSTERS IN SOL–GEL SILICA FILMS FOR SINGLE-WALLED CARBON NANOTUBE GROWTH. Nano, 2009, 04, 99-106.	1.0	5
402	Study of Charge Diffusion at the Carbon Nanotubeâ^'SiO ₂ Interface by Electrostatic Force Microscopy. Journal of Physical Chemistry C, 2009, 113, 15476-15479.	3.1	5
403	Demonstration of 40-nm Channel Length Top-Gate p-MOSFET of WS ₂ Channel Directly Grown on SiO\$_{{x}}\$ /Si Substrates Using Area-Selective CVD Technology. IEEE Transactions on Electron Devices, 2019, 66, 5381-5386.	3.0	5
404	Monolithic Heterogeneous Integration of BEOL Power Gating Transistors of Carbon Nanotube Networks with FEOL Si Ring Oscillator Circuits. , 2019, , .		5
405	Additive manufacturing assisted van der Waals integration of 3D/3D hierarchically functional nanostructures. Communications Materials, 2020, $1, .$	6.9	5
406	Reliability of Ultrathin High-Î $^{ m 0}$ Dielectrics on Chemical-vapor Deposited 2D Semiconductors. , 2020, , .		5
407	Hot carriers in epitaxial graphene sheets with and without hydrogen intercalation: role of substrate coupling. Nanoscale, 2014, 6, 10562-10568.	5.6	4
408	Precision Chemistry in Two-Dimensional Materials: Adding, Removing, and Replacing the Atoms at Will. Accounts of Materials Research, 2021, 2, 863-868.	11.7	4
409	Alloy-buffer-controlled van der Waals epitaxial growth of aligned tellurene. Nano Research, 2022, 15, 5712-5718.	10.4	4
410	Mid-infrared luminescence from coupled quantum dots and wells. Physica E: Low-Dimensional Systems and Nanostructures, 2004, 21, 341-344.	2.7	3
411	Graphitic carbon film formation under Ni templates by radio-frequency sputtering for transparent electrode applications. Journal of Vacuum Science and Technology B:Nanotechnology and Microelectronics, 2011, 29, .	1.2	3
412	A numerical study of Si-TMD contact with n/p type operation and interface barrier reduction for sub-5 nm monolayer MoS ₂ FET. , 2016, , .		3
413	High-Accuracy Deep Neural Networks Using a Contralateral-Gated Analog Synapse Composed of Ultrathin MoSâ,, nFET and Nonvolatile Charge-Trap Memory. IEEE Electron Device Letters, 2020, 41, 1649-1652.	3.9	3
414	Nonvolatile molecular memory with the multilevel states based on MoS ₂ nanochannel field effect transistor through tuning gate voltage to control molecular configurations. Nanotechnology, 2020, 31, 275204.	2.6	3

#	Article	IF	CITATIONS
415	Switchable NAND and NOR Logic Computing in Single Triple-Gate Monolayer MoS2 n-FET. , 2020, , .		3
416	Growth of copper on diatom silica by electroless deposition technique. Materials Science-Poland, 2013, 31, 226-231.	1.0	2
417	Properties and Applications of 2-Dimensional Layered Materials. ECS Journal of Solid State Science and Technology, 2016, 5, Y7-Y7.	1.8	2
418	Performance Limits and Potential of Multilayer Graphene–Tungsten Diselenide Heterostructures. Advanced Electronic Materials, 0, , 2100355.	5.1	2
419	Impact of Schottky Barrier on the Performance of Two-Dimensional Material Transistors. , 2020, , .		2
420	Liquid-phase catalytic growth of graphene. Journal of Materials Chemistry C, 2022, 10, 571-578.	5.5	2
421	Nanoscale Electronic Transparency of Wafer-Scale Hexagonal Boron Nitride. Nano Letters, 2022, , .	9.1	2
422	Grain size effect of monolayer MoS2 transistors characterized by second harmonic generation mapping. , 2015, , .		1
423	Coherent quantum dynamics of excitons in monolayer transition metal dichalcogenides. Proceedings of SPIE, 2016, , .	0.8	1
424	Bioinspired Dimensional Transition: Structurally Deformed MoS ₂ for Electrochemically Stable, Thermally Resistant, and Highly Efficient Hydrogen Evolution Reaction (Adv. Mater. 44/2017). Advanced Materials, 2017, 29, .	21.0	1
425	2D Materials: Metalâ€Guided Selective Growth of 2D Materials: Demonstration of a Bottomâ€Up CMOS Inverter (Adv. Mater. 18/2019). Advanced Materials, 2019, 31, 1970132.	21.0	1
426	Ferroelectric Switching: Giant Ferroelectric Resistance Switching Controlled by a Modulatory Terminal for Lowâ€Power Neuromorphic Inâ€Memory Computing (Adv. Mater. 21/2021). Advanced Materials, 2021, 33, 2170167.	21.0	1
427	Directly Visualizing Photoinduced Renormalized Momentum-Forbidden Electronic Quantum States in an Atomically Thin Semiconductor. ACS Nano, 2022, 16, 9660-9666.	14.6	1
428	Mid-infrared electroluminescence from coupled quantum dots and wells. Journal of Applied Physics, 2004, 96, 2725-2730.	2.5	0
429	Tunning electrical characteristics for networked carbon nanotube field-effect transistors using thiolated molecules. , 2008, , .		0
430	Interaction between fluorene-based polymers and carbon nanotubes/carbon nanotube field-effect transistors. , 2008, , .		0
431	Chapter 3. Photoelectrical Responses of Carbon Nanotube–Polymer Composites. RSC Nanoscience and Nanotechnology, 2013, , 51-71.	0.2	0
432	Fast visible-light phototransistor using CVD-synthesized large-area bilayer WSe <inf>2</inf> ., 2014, , .		0

#	Article	IF	CITATIONS
433	Novel functional devices of transition metal dichalcogenide monolayers. , 2014, , .		0
434	Monolayer MoS2 for nonvolatile memory applications. , 2016, , .		0
435	2D Materials: Single Atomically Sharp Lateral Monolayer pâ€n Heterojunction Solar Cells with Extraordinarily High Power Conversion Efficiency (Adv. Mater. 32/2017). Advanced Materials, 2017, 29, .	21.0	0
436	Synthesis of Transition Metal Dichalcogenides. , 0, , 344-358.		0
437	Observation of Wigner crystal phase and ripplon-limited mobility behavior in monolayer CVD MoS2with grain boundary. Nanotechnology, 2018, 29, 225707.	2.6	0
438	Mapping Strain and Relaxation in 2D Heterojunctions with Sub-picometer Precision. Microscopy and Microanalysis, 2018, 24, 1588-1589.	0.4	0
439	High Performance WSe <inf>2</inf> Transistors with Multilayer Graphene Source/Drain. , 2018, , .		0
440	Thermoelectrics: A Nanostructuring Method to Decouple Electrical and Thermal Transport through the Formation of Electrically Triggered Conductive Nanofilaments (Adv. Mater. 28/2018). Advanced Materials, 2018, 30, 1870243.	21.0	0
441	2D Materials Characterization: Should We Rely on HR STEM Imaging?. Microscopy and Microanalysis, 2019, 25, 1638-1639.	0.4	0
442	Giant Electroresistance Switching of Two-dimensional Ferroelectric $\hat{I}\pm$ -In2Se3 on p+-Si. , 2020, , .		0
443	Uncovering Atomic and Nano-scale Deformations in Two-dimensional Lateral Heterojunctions. Microscopy and Microanalysis, 2020, 26, 1630-1631.	0.4	0
444	Selective Conversion of Carbon Dioxide to Formate with High Current Densities. Journal of Molecular and Engineering Materials, 0, , 2150001.	1.8	0
445	Van der Waals Heterostructures: Temperatureâ€Dependent Electronic Groundâ€State Charge Transfer in van der Waals Heterostructures (Adv. Mater. 29/2021). Advanced Materials, 2021, 33, 2170229.	21.0	0
446	Photoluminescence Enhancement in Defect Monolayer MoSe2 by Hydrohalic Acid Treatment. , 2016, , .		0
447	Epitaxial growth of a 2D transition metal dichalcogenide lateral heterojunction. SPIE Newsroom, 0, , .	0.1	0
448	Circular Polarized Emission of Tungsten Diselenide (WSe2) Atomic Layers with Plasmonic Metasurface. , 2018, , .		0
449	Spectroscopic signature of chiral phonons in 2D materials. , 2018, , .		0
450	Experimental observation of chiral phonons in monolayer WSe2. , 2019, , .		0

#	Article	IF	CITATIONS
451	Electric-field-induced metal-insulator transition and quantum transport in large-area polycrystalline <mml:math xmlns:mml="http://www.w3.org/1998/Math/MathML"><mml:msub><mml:mi>MoS</mml:mi><mml:mn>2monolayers. Physical Review Materials, 2022, 6.</mml:mn></mml:msub></mml:math 	ml:mñ;4/m	ıml:msub>